

Enabling 6G Performance in the Upper Mid-Band by Transitioning From Massive to Gigantic MIMO

Emil Björnson, Ferdi Kara, Nikolaos Kolomvakis, Alva Kosasih, Parisa Ramezani, and Murat Babek Salman

Abstract—The initial 6G networks will likely operate in the upper mid-band (7-24 GHz), which has decent propagation conditions but underwhelming new spectrum availability. In this paper, we explore whether we can anyway reach the ambitious 6G performance goals by evolving the multiple-input multiple-output (MIMO) technology from being massive to gigantic. We describe how many antennas are needed and can realistically be deployed, and what the peak user rate and degrees-of-freedom (DOF) can become. We further suggest a new deployment strategy that enables the utilization of radiative near-field effects in these bands for precise beamfocusing, localization, and sensing from a single base station site. Finally, we identify five open research challenges that must be overcome to efficiently use gigantic MIMO dimensions in 6G from hardware, cost, and algorithmic perspectives.

Massive multiple-input multiple-output (mMIMO) technology has been fundamental to fifth-generation (5G) wireless networks, which use it for beamforming, interference suppression, and spatial multiplexing [1]. mMIMO has enabled higher user data rates and increased network capacity by greatly improving spectral efficiency compared to fourth-generation (4G) networks. The commercialization of mMIMO in 5G has been successful: at the end of 2023, mobile network operators (MNOs) provided mMIMO 5G coverage to 45% of the world’s population [2].

Present 5G deployments mainly use lower mid-band frequencies in the 3.5 GHz band and continue to expand worldwide. The next step is to utilize the 6.5 GHz band, which was recently identified for worldwide use by the International Telecommunications Union (ITU) [3]. Meanwhile, the research into the next generation of wireless communication systems, known as 6G, is about to shift towards standardization and technology development. Evidently, 6G must provide more capacity to meet the ever-increasing traffic demands and enable new data-intensive applications such as virtual reality, augmented reality, and ultra-high-definition video streaming. To achieve commercial viability, 6G must also support new use cases and functionalities and ensure connectivity for many more devices with diverse characteristics. Previous generational shifts have been associated with wider bandwidths at higher carrier frequencies because more spectrum directly

leads to higher rates. In the last decade, it was believed that the millimeter-wave (mmWave) band (24 GHz and above) would be the natural next step due to the abundant spectrum availability. In fact, 5G was co-designed for two frequency ranges (FRs): FR1 with 0.4-7 GHz and FR2 with 24-71 GHz. However, the intermittent coverage caused by high susceptibility to blockage in mmWave bands presents a significant challenge, requiring expensive dense small-cell deployments to address. In light of these issues, the MNOs in South Korea closed their commercial mmWave networks in 2023. While the research community is actively investigating even higher bands, called terahertz (THz) and sub-THz, these will inherit and worsen the challenges and limitations of mmWave frequencies.

Towards this background, there is a growing interest from academia and industry in the missing interval along the frequency axis: the *upper mid-band* from 7-24 GHz (also known as FR3) [4], [5]. This band is nowadays known as the *Golden Band* for 6G due to its promising balance between bandwidth availability and coverage [6]. The 6G standardization begins in 2024 and will finish by 2028-2029, so commercial 6G networks can open in 2029-2030. These networks will likely operate in the upper mid-band. Although the channel characteristics, coexistence with existing services, and coverage assessment in this new band were recently reviewed in [4]–[7], the assessments of MIMO in these new bands are yet to explore.

This paper describes why major enhancements in the MIMO technology is the key to delivering the promised 6G performance enhancements. Although mMIMO originally referred to systems with an unlimited number of antennas [8], the term is nowadays used commercially to describe MIMO configurations with 16, 32, or 64 antenna ports in 5G. The recent research literature contains alternative terms associated with MIMO in THz, continuous apertures, or extremely large physical sizes—none of which is the topic of this paper. Therefore, we think a new commercial MIMO term is needed to refer to 6G MIMO in the upper-mid band, and we propose the term *gigantic MIMO (gMIMO)*.

In the remainder, we first briefly review the prospective 6G bands and their characteristics and then elaborate on how many antennas we need to use in the upper mid-band. We further describe how gMIMO can enable enormous peak rates and discuss the practically achievable performance. We then shift focus to the radiative near-field and how its previously unused characteristics might enable beamfocusing

The authors are with the KTH Royal Institute of Technology, Sweden, and have contributed equally. F. Kara is also with Zonguldak Bülent Ecevit University, Türkiye. This work is supported by the Swedish Foundation for Strategic Research and the SweWIN Vinnova Competence Center.

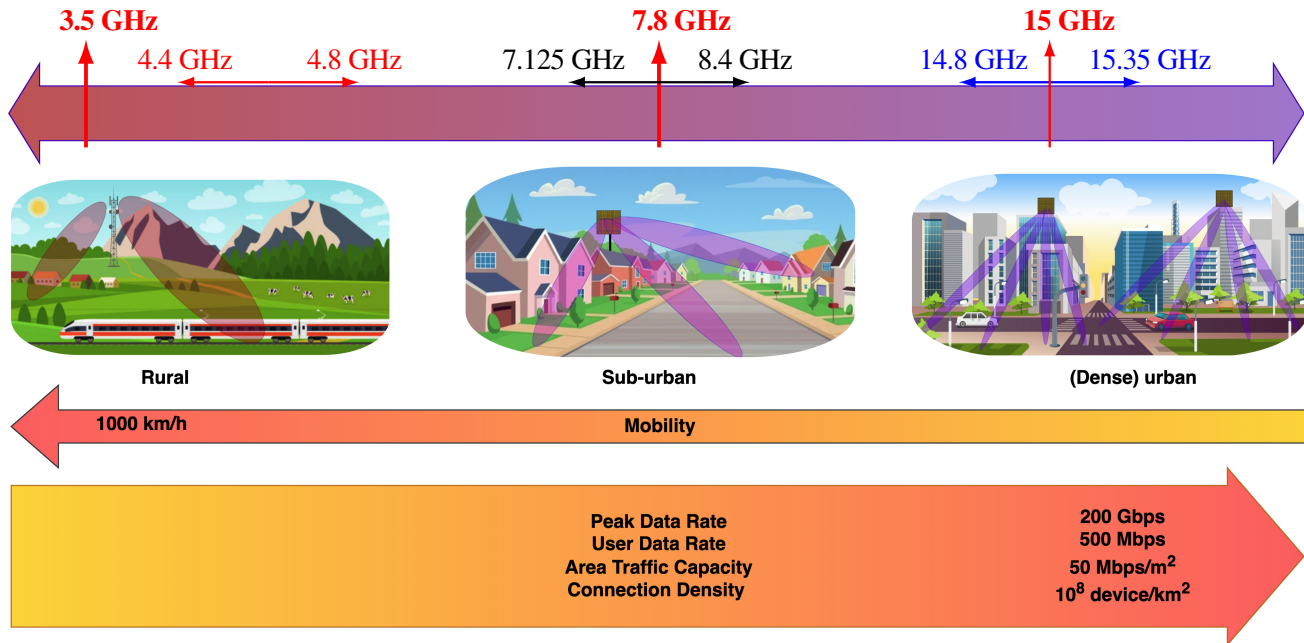


Fig. 1: Towards gMIMO: New spectrum for 6G and related IMT 2030 targets in these bands.

and precise localization in 6G. Finally, we identify unexplored research challenges whose solutions could greatly impact 6G standardization and implementation.

CANDIDATE 6G BANDS AND THEIR FEATURES

The ITU harmonizes the worldwide spectrum utilization, which is vital for efficiently deploying new wireless technologies, ensuring compatibility and interoperability across various regions. ITU calls cellular network technology *International Mobile Telecommunications (IMT)* and has published its IMT-2030 vision for 6G [9]. This section will briefly describe the specific 6G bands proposed by the ITU-organized World Radiocommunication Conference 2023 (WRC-23) and their properties compared to 5G bands.

Candidate 6G Bands Identified by ITU: By considering factors such as the anticipated technological advancements and IMT-2030 vision, regional conflicts over existing wireless services, and demands from industrial stakeholders, WRC-23 identified three candidate bands (one from FR1 and two from FR3) for 6G in addition to the continued use of legacy 5G bands [3]. These bands are as follows, where ITU Region 1 includes Europe, Middle East, and Africa, Region 2 includes the Americas, and Region 3 includes East Asia and Oceania.

- **4.4-4.8 GHz (Regions 1 and 3):** This additional sub-7 GHz band was requested by industrial stakeholders to provide extensive coverage and support high mobility in suburban and rural areas.
- **7.75-8.4 GHz (Region 1) and 7.125-8.4 MHz (Regions 2 and 3):** This upper mid-band frequency is intended for outdoor-indoor applications in urban and suburban areas to meet high data rate and modest mobility requirements.
- **14.8-15.35 GHz (All ITU regions):** This upper mid-band allocation is primarily for dense-urban and urban areas

to meet massive connectivity and high data rate needs under relatively low user mobility.

The per-band use cases are illustrated in Fig. 1. Importantly, not all IMT-2030 visions must be reached in all bands.

Coexistence and Interference Management: Before any candidate bands can be assigned for 6G, further technical studies must be conducted to determine if the intended performance can be reached while ensuring coexistence with existing services, such as broadcast satellites and feeder links for satellite communication. These issues are detailed in [4], [6], [7]. Traditional coexistence solutions rely on spectrum masks, antenna tilting, and cognitive radio. Next-generation MIMO technology could offer a more flexible solution with extremely narrow directional beams and real-time out-of-system interference suppression. ITU aims to finalize the technical studies by the next WRC in 2027, the last WRC before the intended 6G roll-out in 2030.

Spectrum Availability: The three new bands contain 400 MHz, 650-1275 MHz, and 550 MHz bandwidths, respectively. The total spectrum is 1600-2225 MHz, depending on the region. These numbers should be compared to the 500 MHz of the current 5G mid-band spectrum in the range 3.3-3.8 GHz (the exact numbers vary between regions), plus the new 700 MHz of spectrum in the range 6.4-7.1 GHz assigned for 5G at WRC-23. Hence, the first 6G BSs using one of the above-mentioned new bands will offer roughly as much new spectrum as the 5G networks in 2029 already have aggregated. This demonstrates how increased spectrum availability will not be the main distinguishing factor between 6G and 5G.

The ITU vision for 6G is a peak user data rate of 200 Gbps, guaranteed rate of 500 Mbps, and area traffic capacity of 50 Mb/s/m² [9]. Suppose 1.2 GHz of new spectrum is available,

then a peak spectral efficiency of 166 b/s/Hz is required to reach the envisioned peak rate. This can only be achieved through major advances in the MIMO technology.

Balanced Propagation Characteristics: The upper mid-band frequencies offer a balance between capacity and coverage. They can penetrate buildings more effectively than mmWave frequencies (FR2) and provide moderate propagation losses similar to FR1 bands [10] so that comprehensive urban and suburban coverage can be achieved with a cost-efficient number of beamforming-capable BSs.

HOW MANY ANTENNAS

DO WE WANT IN 6G BASE STATIONS AND DEVICES?

Increasing the carrier frequency is often said to generate higher pathlosses, but the reality is more complex because pathloss formulas always depend on both the transceiver hardware and wireless propagation. Understanding this interplay is essential when designing 6G systems operating at higher frequencies than in 5G but with similar coverage.

Suppose the transmitter and receiver have antenna arrays with the effective areas A_t and A_r , respectively. In a free-space line-of-sight (LOS) scenario, the received power is $P_t A_r A_t / (d\lambda)^2$, which depends on the transmit power P_t , propagation distance d , and wavelength λ [1]. If the array areas are fixed, the received power increases quadratically with the carrier frequency because λ shrinks accordingly. Hence, it is better to operate at higher frequencies than lower ones. To realize this result in practice, we must use antenna arrays with antenna numbers growing as $1/\lambda^2$ since the area of an individual fixed-gain antenna is proportional λ^2 . For example, if the wavelength is halved (doubling the frequency), the effective area of each antenna element is reduced by a factor of four. Thus, to compensate, we need four times as many antenna elements to obtain the same total area.

This observation contradicts the opposite claim mentioned at the beginning of this section. To reach the opposite result, one must consider a bad system design (e.g., with a fixed number of antennas) or non-LOS scenarios with materials that cause propagation losses that grow rapidly with frequency. The latter is the main practical showstopper for mmWave networks.

A reasonable design goal is to keep the free-space pathloss constant as the frequency increases, allowing us to reduce the array areas such that $A_t A_r \sim \lambda^2$. For instance, we can let the BS maintain its array area while the user equipment (UE) keeps its antenna number fixed. Fig. 2 shows the multiplicative factor for the number of BS antennas that achieve the same pathloss at a carrier frequency f_c as in a baseline case of $f_0 = 3.5$ GHz. There are curves for the cases with a fixed number of UE antennas and $2\times$ or $4\times$ more antennas than in the baseline. A BS in the 7.8 GHz band or 15 GHz band can have up to 5 or 18 times more antennas,

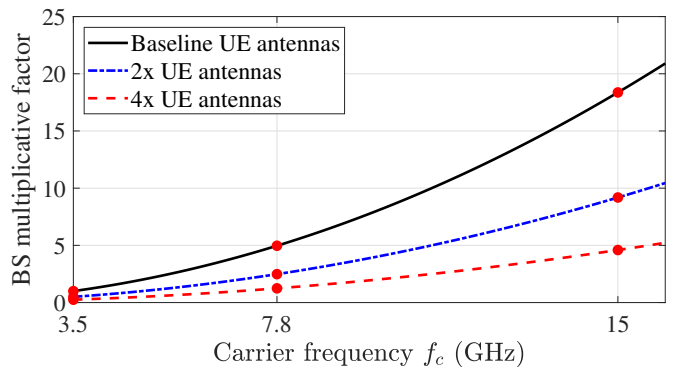


Fig. 2: The multiplicative factor for the number of BS antennas versus the carrier frequency. It expresses how many times more BS antennas are needed to maintain the same free-space pathloss as at 3.5 GHz. The value depends on whether we scale the number of UE antennas.

respectively, than in current 5G networks. If the UE doubles or quadruples its antenna elements, these numbers reduce to $1.2\times$ - $2.5\times$ and $4.6\times$ - $9.2\times$, respectively.

Even if the number of antenna elements grows quadratically with the carrier frequency, the physical size will not increase. Fig. 3 illustrates this fact for an array of dimensions $0.5\text{ m} \times 0.5\text{ m}$, which resembles current 5G BSs. With a typical half-wavelength-spacing, this area fits 121 dual-polarized antenna elements at 3.5 GHz, 625 elements at 7.8 GHz, and 2304 elements at 15 GHz. The number of antenna ports (transceiver branches) might be around 33% of this because the industry usually connects each port to a group of 2-4 elements to limit the number of hardware components. Regardless, the MIMO dimensions evolve from being *massive* to *gigantic*, motivating the new gMIMO terminology in 6G.

The pathloss discussion above only captures one MIMO functionality: beamforming. If we shift focus to spatial multiplexing, the spatial DOF are limited by the number of UE antennas. Even if not needed from a pathloss perspective, we can add more UE antennas to achieve higher DOF, which typically leads to higher user rates. On the other hand, from a channel estimation perspective, having many antennas only on one side (i.e., the BS) is advantageous because the estimation overhead is proportional to the minimum number of antennas at the transmitter and receiver [1]. Hence, there is a non-trivial trade-off and the preferred solution is scenario-dependent: the richness of the multipath environment determines how many large singular values can be achieved, and user mobility determines how many resources can be dedicated to channel estimation.

Increasing the number of antenna elements also impacts the beamwidth of the signals transmitted and received by the array. The half-power beamwidth, which is the angular interval where the radiation pattern is at least 50% of its peak value, becomes narrower as the number of antenna elements increases. If we keep the array dimensions constant, the beamwidth is

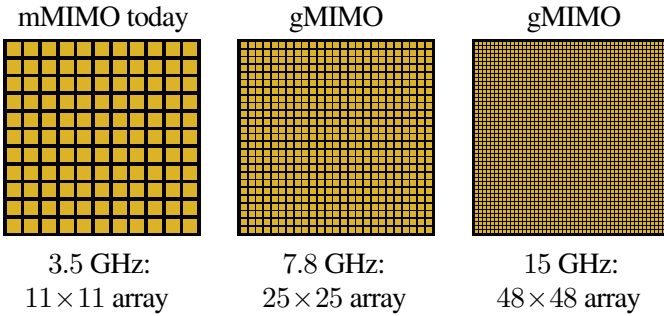


Fig. 3: Comparison of three arrays of the size $0.5\text{m} \times 0.5\text{m}$ using different carrier frequencies. The number of half-wavelength-spaced antennas that fit into this aperture grows quadratically with the frequency.

proportional to the wavelength so that it will be $2.2\times$ smaller at 7.8 GHz and $4.3\times$ smaller at 15 GHz compared to the 3.5 GHz band. The increased directionality reduces interference to/from unwanted directions but increases the need for precise and timely channel estimation. This is cumbersome both for digital transceivers that cannot rely on beamforming gains during channel estimation and for hybrid transceivers that require sophisticated tracking and beam-steering technologies to maintain robust communication links under mobility.

Finally, two good reasons exist for not keeping the free-space pathloss constant when moving to the upper mid-band but improving it by maintaining the array areas on both sides. Firstly, we might want a pathloss margin to handle larger non-LOS losses. Secondly, the signal-to-noise ratio (SNR) is inversely proportional to the bandwidth. If we cannot afford to increase the transmit power in 6G systems—even if we have more bandwidth—the extra beamforming gain comes in handy. This is particularly important in the uplink.

ACHIEVABLE RATES IN PROSPECTIVE 6G BANDS

The user rates that can be achieved in a specific band vary enormously between the theoretical peak values and the average or guaranteed values under practical conditions. In this section, we will elaborate on both aspects to the prospective 6G bands in FR3.

The theoretical peak rate is computed as the product of the bit rate per symbol, the spatial DOF, and the bandwidth. Starting with the former, 5G supports up to 1024-QAM, while WiFi 7 also handles 4096-QAM. Assuming that 6G follows this development, we can reach 12 bit/symbol. Moreover, a current 5G device has 4 antennas, which might increase by $4\times$, leading to 16 spatial DOF. Finally, if a single operator uses all 1.2 GHz of spectrum in the 7.8 GHz band, we will reach $12 \cdot 16 \cdot 1.2 = 230$ Gbps. Hence, the ITU vision of 200 Gbps is within theoretical reach but only by combining enormous spatial multiplexing with greatly expanded bandwidths. The peak rate is reduced by one-third if the available bandwidth is divided between three MNOs.

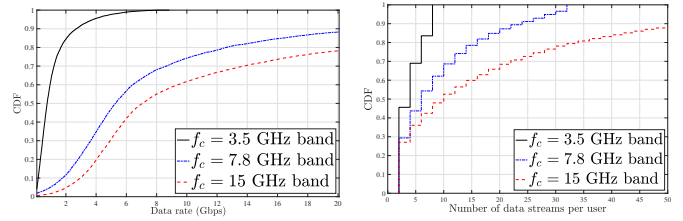


Fig. 4: CDFs of the per-user data rate and per-user data streams (spatial multiplexing) for 3GPP Urban Micro Cell LOS

Still, the gMIMO gains remain feasible and essential for making 6G user rates significantly larger than in 5G.

The upper mid-band is claimed to be a golden opportunity for maintaining the favorable coverage characteristics of sub-7 GHz bands while delivering typical user rates resembling or surpassing those in mmWave bands. To evaluate this claim, we have simulated a realistic propagation scenario. We can surely fit more antennas into a BS and device in FR3 than in FR1 to obtain higher beamforming gains. However, will the propagation be sufficiently favorable to obtain higher DOF per UE?

We will compare the downlink user rates achievable in the new 7.8 and 15 GHz bands, shown in Fig. 1, with the current 3.5 GHz bands. The size of the BS array is fixed to $0.5\text{m} \times 0.5\text{m}$; hence, the number of half-wavelength-spaced dual-polarized antennas increases with the carrier frequency. We consider 10 UEs, each equipped with an antenna array of size $4\text{cm} \times 4\text{cm}$. The QuaDRiGa model developed at Fraunhofer HHI was used to generate realistic channel realizations for an urban microcell scenario. The users are randomly distributed in a $1\text{km} \times 1\text{km}$ area around the BS. The left part of Fig. 4 presents the cumulative distribution function (CDF) of the user rates obtained at different locations. We consider LOS scenarios and assume 400 MHz user bandwidth for upper mid-band frequencies and 100 MHz for sub-6 GHz frequencies. The transmit power of the BS is adjusted such that 1 W is supplied per 1 MHz bandwidth. Perfect channel state information (CSI) at the BS is assumed, and block diagonalization precoding based on water-filling power allocation is performed.

The results presented in Fig. 4 demonstrate that the utilization of new frequency bands can significantly enhance capacity for LOS scenarios compared to the sub-7 GHz bands. 1 Gbps is guaranteed to almost all UEs, and many achieve more than 10 Gbps. This improvement is primarily due to the increased beamforming gain, which is facilitated by the ability to deploy a larger number of antennas in these new frequency bands. The performance aligns with the anticipated requirements for future 6G systems, which aim to guarantee 500 Mbps to everyone. Due to the limited number of antennas that can be accommodated in the 3.5 GHz band, its capability to mitigate multi-user interference is constrained. Therefore, the new upper mid-band frequency shows promise for achieving improved capacity performance thanks to its

ability to support more simultaneous user streams for LOS channels. Furthermore, the number of data streams that can be transmitted to each UE is investigated in the right part of Fig. 4. It is seen that the 2 stream per user (1 for each polarization) is sufficient for most UEs at 3.5 GHz. However, as the carrier frequency increases, more data streams can be provided per UE, which explains the shape of the curves in Fig. 4 (right). For the 7.8 GHz band, up to 16 data streams, and for the 15 GHz band, up to 64 data streams for each polarization can be supported. These results demonstrate that higher DOF is achieved in practice when increasing the number of UE antennas, even if the array area is constant. While there is a considerable enhancement in potential spatial multiplexing for individual users, the capacity improvement resulting from approximately doubling the center frequency from 3.5 GHz to 7.8 GHz is more significant than a comparable relative increase from 7.8 GHz to 15 GHz, primarily due to pathloss and available bandwidth. Consequently, the candidate bands under examination demonstrate the potential for sophisticated management of coverage and capacity trade-offs. Note that the number of users is fixed at 10 for this analysis, while in scenarios involving higher frequency bands, the potential for gMIMO to serve many more users becomes evident. This enhancement both improves the overall system performance and accentuates the advantages of operating within the upper mid-band frequencies, making them particularly attractive for advanced wireless communication systems.

NEAR-FIELD COMMUNICATIONS

The beamwidth shrinks with the carrier frequency, as previously mentioned, but also the shape of the beam in the transverse propagation direction can change. This phenomenon is associated with the so-called radiative near-field, which is the region where the wavefront's spherical curvature is noticeable. The far-field region with approximately planar wavefronts begins at the Fraunhofer distance, calculated as $2D_{\text{array}}^2/\lambda$, where D_{array} is the aperture length of the transmitter array [11]. When the aperture is physically large or the wavelength is tiny, the Fraunhofer distance can become big and we observe near-field propagation conditions when serving UEs at shorter distances. This is not the case in 5G, but we will explore if it happens in 6G.

When a beam is focused on a near-field location, the transverse variations in spherical curvature dissolve the focusing after a particular distance. Consequently, in the near-field, the beampattern resembles a spotlight, as opposed to the far-field pattern that disperses as a cone across space [11]. One significant advantage of such *near-field beamfocusing* is that a gMIMO system can distinguish between user devices and multipath clusters in the distance domain, in addition to the angular domain. This feature makes multi-user MIMO channels appear richer and enhances the sum capacity [12].

To explore the presence of such near-field effects in the prospective 6G bands, we plot the relative beamforming gain (from 0 to 1) observed in the azimuth plane in the middle figure of Fig. 5. The BS is equipped with a uniform linear array (ULA) composed of $N = 48$ half-wavelength-spaced antennas operating at the 15 GHz carrier frequency. This corresponds to the array in Fig. 3 but with one transceiver branch per column since we consider a two-dimensional setup. The BS is at the origin and focuses a beam on a UE 30 m away in the broadside direction. We observe that the beam energy spreads out infinitely behind the UE. This is a typical far-field beampattern and was expected since the UE distance is larger than the Fraunhofer array distance of 23 m.

To achieve near-field beamfocusing, we can increase the number of antennas in the array, thereby expanding the aperture length and Fraunhofer distance. This is undesirable from a deployment and complexity perspective. Alternatively, we can shift the carrier frequency to the mmWave band (as in [12]), but that is undesirable due to the poor coverage.

There is one realistic way to exploit near-field beamfocusing in 6G: We can divide the array into smaller subarrays and deploy them at the same location but some meters apart. We can perform coordinated multi-array transmission and benefit from the expanded distance between the outermost antennas. To demonstrate this possibility, we consider two subarrays with 24 antennas, so the total number is 48. The two arrays are separated by 5 m and focus the signal at the same UE location as before. The corresponding beampattern is depicted in the right hand figure of Fig. 5 and shows a precise beamfocusing effect at the desired location with minor energy leakage to the surrounding area.

These results suggest a new 6G deployment strategy for urban scenarios: instead of one conventionally-sized BS panel, we can deploy multiple smaller panels separated by many meters on the same rooftop. They operate as a single BS and use a common baseband processing unit. This can be viewed as the first step towards the cell-free mMIMO architecture [1], where the arrays are distributed over large areas and require additional fronthaul and synchronization infrastructure.

NEAR-FIELD LOCALIZATION AND SENSING

6G is envisioned to expand its functionality beyond connectivity and become an integrated communication, localization, and sensing service platform. So far, we have demonstrated how gMIMO enables communication improvements in the upper mid-band spectrum, but can we also enable precise localization and environmental awareness? We will analyze these prospects in this section.

In the far-field, an antenna array can estimate the angle of a source transmitting a narrowband signal but not the distance since the planar wavefront lacks such information. By contrast, when the sources are within the radiative

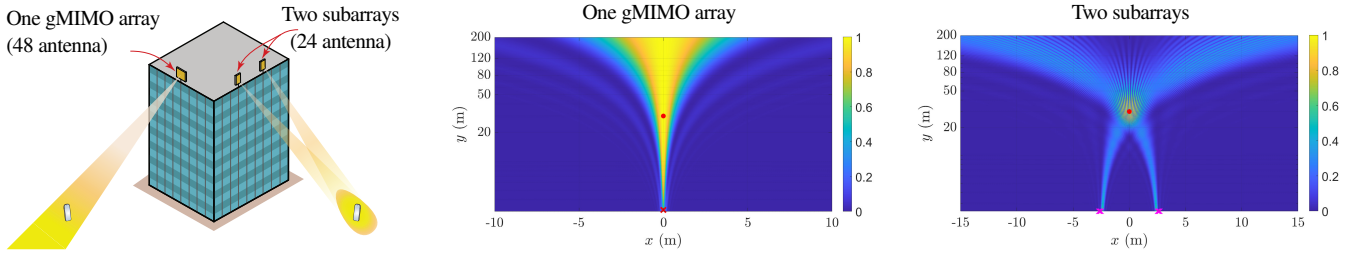


Fig. 5: Beam patterns in the upper mid-band depending on the array configuration. The transmitter array locations are indicated with magenta (\times), while red (\circ) indicates the UE location (focal point). These simulation setups are given in the sketch.

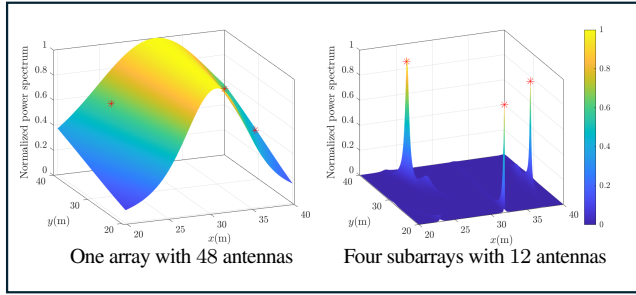


Fig. 6: The MUSIC power spectra for localization of three sources.

near-field region of the antenna array, high-resolution three-dimensional location estimation can be achieved by capturing both angle and distance information from the impinging spherical wavefronts [13]. These near-field features can be easily utilized in mmWave and sub-THz bands where the wavelength is tiny; however, the end of the near-field region (i.e., Fraunhofer distance) is only some tens of meters for a conventionally-sized 6G BS in the upper mid-band.

In the previous section, we highlighted that coordinated subarrays deployed with a few meters of separation enable near-field beamfocusing without requiring a huge continuous aperture. We will now demonstrate that localization can also benefit from this new deployment strategy. The individual subarrays observe locally planar wavefronts, but the spherical curvature is observable when fusing the received signals from multiple arrays.

Fig. 6 considers localization of three sources at the carrier frequency of 15GHz using the well-known Multiple Signal Classification (MUSIC) algorithm. We consider either one ULA with 48 half-wavelength-spaced antennas or the same number of antennas divided between four subarrays 5 m apart, deployed similarly to Fig. 5. The left figure shows the normalized power spectrum with one ULA. The MUSIC algorithm will fail to localize the sources since there are no peaks at their locations. This is expected since the sources are far beyond the Fraunhofer distance [11] and closely spaced in angle. Therefore, the received signal looks like a single planar wave from which only one angle can be extracted.

The right figure shows the corresponding power spectrum

with four subarrays. We can see that the locations are accurately detected in this scenario thanks to the near-field propagation effects that the subarrays can jointly observe. Specifically, the phase variations across the subarrays depend on each source's exact location due to the spherical wavefronts and make it possible to resolve the locations accurately.

In a nutshell, near-field localization using a single array necessitates an inconveniently large array in the upper mid-band due to the relatively large wavelength. Nevertheless, we can enable near-field localization using multiple small subarrays displaced by a few meters and processed jointly. Similarly, for radar sensing, one subarray can form beams toward passive targets and the other subarrays can detect their locations in a multi-static fashion with high angle and distance resolution. This new deployment strategy is clearly suitable for integrated 6G near-field communication, localization, and sensing.

OPEN RESEARCH CHALLENGES

Since the mid-band spectrum is limited, 6G must transition from mMIMO to gMIMO to deliver better services than 5G. This section outlines research challenges that must be overcome to enable this development.

Near-field antenna placement strategies and compliant models: We have demonstrated that communication and localization performance can be significantly enhanced by leveraging the near-field beamfocusing effect, which requires a sufficiently large array aperture when operating in the upper mid-band spectrum. This can be achieved through widely spaced subarrays, as previously shown, or alternatively futuristic movable antennas offering dynamic configurations for specific tasks [14]. Both the subarray and movable antenna approaches introduce irregularities in the array geometry, affecting algorithms that rely on the array response vector, which depends on both angle and distance in the near-field. Additionally, no widely accepted near-field channel models exist. Addressing these challenges will require measurements, enhanced ray-tracing, and machine learning (ML) to develop minimally complex models that capture spherical wavefront propagation and interactions with the environment. These models will be used to refine MIMO signal-processing algorithms to effectively exploit these features.

Medium-resolution transceivers and computations: We need more antennas to maintain a decent pathloss in the upper mid-band, and many transceiver branches to control them. Since hybrid analog/digital transceivers are unsuitable for multi-user scenarios and one-bit digital transceivers cannot coexist well with other systems, we need a new generation of medium-resolution MIMO transceivers. Lowering the hardware resolution by just a few steps can drastically reduce cost and energy consumption, at the expense of non-linear phase injections, amplification, and calibration errors. This calls for new algorithms, possibly empowered by ML to track hardware characteristics. Moreover, the multi-user beamforming complexity grows cubically with a fixed antenna/user ratio [1], which might be managed through novel compression and offloading methods.

Resource-efficient channel estimation: Beamforming and spatial multiplexing require timely and precise CSI, most efficiently acquired by sending one distinct pilot sequence per DOF per coherence time [1]. We need longer pilots to accommodate more DOF in 6G, but coherence time generally shrinks with wavelength. New resource-efficient estimation is needed to overcome this challenge, possibly via pilot reuse within each cell and addressing the resulting contamination algorithmically.

Information-theoretic capacity limits: The theoretical MIMO foundations are deep for single-antenna UEs [1], but there are many open problems for scenarios with multi-antenna UEs. What are the DOF of a noncoherent MIMO system with structured channels? The seminal work [15] only covers isotropic fading, which is a very pessimistic assumption, yet we follow its guidelines when designing current networks. What kind of waveform and combination of data/reference signals are sufficient to fully exploit these DOF? Is there a need for non-linear processing or rate-splitting methods?

Energy efficiency optimization: gMIMO has promising implications for enhancing energy efficiency by compensating for the increased energy consumption of additional antenna-hardware with significantly higher data rates. However, more detailed studies are needed to fully understand these gains. Furthermore, while coordinated multi-array transmission and localization improve coverage and accuracy without adding more antennas, the synchronization between sub-arrays may increase energy consumption, making it essential to closely analyze the energy efficiency from many viewpoints.

CONCLUSIONS

The first 6G networks will operate in the upper mid-band with modest spectrum availability but great prospects for huge-dimensional beamforming and spatial multiplexing. We call this paradigm *Gigantic MIMO* and have shown how it

reaches the 6G performance goals. We have demonstrated how distributed subarray deployment enables near-field beamfocusing and localization/sensing. Finally, five pertinent research challenges have been identified.

REFERENCES

- [1] E. Björnson, J. Hoydis, and L. Sanguinetti, "Massive MIMO networks: Spectral, energy, and hardware efficiency," *Foundations and Trends® in Signal Processing*, vol. 11, no. 3-4, pp. 154–655, 2017.
- [2] Ericsson, "Ericsson mobility report," Jun. 2024. [Online]. Available: <http://www.ericsson.com/mobility-report>
- [3] "World Radiocommunication Conference 2023 (WRC-23) – Final Acts," 2023. [Online]. Available: <https://www.itu.int/en/publications/ITU-R/pages/publications.aspx?parent=R-ACT-WRC.16-2024&media=electronic>
- [4] S. Kang, M. Mezzavilla, S. Rangan, A. Madanayake, S. B. Venkatakrishnan, G. Hellboug, M. Ghosh, H. Rahmani, and A. Dhananjay, "Cellular wireless networks in the upper mid-band," *IEEE Open J. Commun. Soc.*, vol. 5, pp. 2058–2075, 2024.
- [5] F. Chaves, D. Chizhik, J. Du, A. Ghosh, B. Love, and E. Visotsky, "Coverage evaluation of 7–15 GHz bands from existing sites," *Nokia White Paper*, Apr. 2024.
- [6] Z. Cui, P. Zhang, and S. Pollin, "6G wireless communications in 7-24 GHz band: Opportunities, techniques, and challenges," *arXiv:2310.06425*, 2023.
- [7] J. Zhang, H. Miao, P. Tang, L. Tian, and G. Liu, "New mid-band for 6G: Several considerations from the channel propagation characteristics perspective," *IEEE Commun. Mag.*, 2024, to appear.
- [8] T. L. Marzetta, "Noncooperative cellular wireless with unlimited numbers of base station antennas," *IEEE Trans. Wireless Commun.*, vol. 9, no. 11, pp. 3590–3600, 2010.
- [9] "Recommendation ITU-R M.2160-0: Framework and overall objectives of the future development of IMT for 2030 and beyond," 2023. [Online]. Available: <https://www.itu.int/rec/R-REC-M.2160/en>
- [10] D. Shakya, M. Ying, T. S. Rappaport, H. Poddar, P. Ma, Y. Wang, and I. Al-Wazani, "Comprehensive FR3 and FR1(C) upper-mid band propagation and material penetration loss measurements and channel models in indoor environment for 5G and 6G," *tehrxiv.171710345.58907668*, 2024.
- [11] P. Ramezani, A. Kosasih, A. Irshad, and E. Björnson, "Exploiting the depth and angular domains for massive near-field spatial multiplexing," *IEEE BITS Inf. Theory Magazine*, vol. 3, no. 1, pp. 14–26, 2023.
- [12] G. Bacci, L. Sanguinetti, and E. Björnson, "Spherical wavefronts improve MU-MIMO spectral efficiency when using electrically large arrays," *IEEE Wireless Commun. Lett.*, vol. 12, no. 7, pp. 1219–1223, 2023.
- [13] P. Ramezani, Ö. T. Demir, and E. Björnson, *Massive MIMO for Future Wireless Communication Systems: Technology and Applications*. Wiley-IEEE Press: Cambridge University Press, 2025, ch. Localization in Massive MIMO Networks: From Near-Field to Far-Field.
- [14] L. Zhu, W. Ma, and R. Zhang, "Movable antennas for wireless communication: Opportunities and challenges," *IEEE Commun. Mag.*, vol. 62, no. 6, pp. 114–120, 2024.
- [15] L. Zheng and D. Tse, "Communication on the Grassmann manifold: a geometric approach to the noncoherent multiple-antenna channel," *IEEE Trans. Inf. Theory*, vol. 48, no. 2, pp. 359–383, 2002.